Workshop between University of Nottingham & Tokyo Polytechnic University,
School of the Built Environment, University of Nottingham, UK
25/26 April 2005

Toward the establishment of research field of "Public Health Engineering"

Development of Indoor Air Quality Prediction Method based on Numerical Simulation

Kazuhide Ito[1] and Yu Mizuno[2]

[1] Wind Engineering Research Center, Tokyo Polytechnic University, Japan
[2] Ph.D Student, Graduate School of Engineering, Tokyo Polytechnic University, Japan

ABSTRACT: The final goal of our study is to establish a paradigm for the integrated design of indoor environment that takes into account the Indoor Air Chemistry, Biology and Physics. In other words, our target is to develop the research field of Public Health Engineering. This paper reports the activity of laboratory of indoor environment and health at Wind Engineering Research Center, Tokyo Polytechnic University, with regard to the research of Public Health Engineering.

Keywords: *Public Health Engineering, Computational Fluid Dynamics, Indoor Air Chemistry, Indoor Air Biology, Indoor Air Physics*

1. INTRODUCTION

Issues on indoor air environments are being shifted from high-concentration and short-term exposure such as suspended particulate matters and carbon monoxide, to low-concentration and long-term exposure typically represented by sick buildings and sick houses syndrome. The first is due to the incomplete combustion of conventional open combustion equipment. The issue of the suspended particulate matters of mg/m^3 order or over is due to environmental tobacco smoke (ETS), etc. The last is due to the very small quantity of volatile organic compounds (VOC). Moreover, microbial contaminants such as molds, fungi, etc. due to damp building issues have complicated the problems of indoor air environments.

The “quality” problem regarding the overall indoor environment is called IEQ (Indoor Environmental Quality). Recently, this area has increasingly attracted attention with the increasing health consciousness of residents. The research project of the laboratory of indoor environment and health at Wind Engineering Research Center (WERC), Tokyo Polytechnic University (TPU), will be based on the analysis of the flow field that is formed indoors and will deal with IEQ control totally. Key words of our research project are Contamination Control and Public Health Engineering.
This research will focus on indoor air pollution issues that have a large influence on the health risk of indoor residents among the IEQ factors. The research fields are physical environmental factors such as indoor airflow, temperature field, humidity field, etc., and microbial contamination due to molds, fungi, etc. and chemical compounds contamination due to volatile organic compounds. Comprehensive research will be carried out on IEQ control from the physical, biological and chemical standpoints focusing on the above areas.

In fact, the conventional approach is to study separately the individual issues of chemical compounds contamination and microbial contamination, and measures are also taken separately. However, the organic compound called MVOC (microorganism-origin volatile organic compound) has recently been measured. It has recently been pointed out that a certain correlation can exist between indoor microbial quantity and concentration of chemical compounds. This implies that indoor chemical compounds contamination due to volatile organic compounds and microbial contamination due to mold, fungi, etc. are closely interrelated. Thus, it does not suggest separate treatment but the need to study the issues by linking both factors. As a matter of course, growth, breeding and metabolizing of microorganism and diffusion characteristics of chemical compounds and airborne fungi are closely related to indoor physical environmental factors (thermal environment, humidity environment, air flow, etc.). Thus, comprehensive measures are necessary.

The laboratory of indoor environment and health, WERC, TPU are carrying out the researches on IEQ control as mentioned above from three aspects: (1) chemical, (2) biological and (3) physical.

(1) Studies dealing with the chemical environment are directed to developing a numerical model that can be the basis of prediction for the indoor chemical compounds concentrations. This is accomplished by measuring the quantity of chemical compounds diffusion, the quantity of adsorption and desorption using flat-plate test chamber, and the quantity of chemical reaction using the room model type chemical-free chamber.

(2) Studies dealing with the biological environment are directed to developing a numerical model of microorganism growth based on measurement of microorganism growth response using a incubator (constant-temperature and constant-humidity test chamber) and to develop the numerical model that predict MVOC emission rate by taking into account the influence of moisture and temperature.

(3) Studies dealing with the physical environment are directed to developing a high accuracy prediction method for the indoor physical environment based on several technique in addition to the analysis of the indoor air flow based on CFD (Computational Fluid Dynamics) technique, analysis of the temperature coupled with convection and radiation heat transfer, analysis of the humidity field including condensation simulation, and analysis of contaminant diffusion and so on. Furthermore, the gird library of Virtual Manikin in which takes into account various attitude, gender and comfort model will be developed for coupled CFD simulation around human body for the analysis of micro-environment.

The final goal of our research project is to establish a high-accuracy IEQ prediction methods based on the CFD simulation technique.

2. INDOOR AIR CHEMISTRY

Many factors, including air change rate and emission, adsorption / desorption, chemical reactions within the source material and the room air, affect the concentration of chemical pollutants within a room. In this study, a method for predicting the distribution of chemical pollutants emitted or transported in a room was investigated. Indoor air quality is greatly affected by the emission, sorption and chemical reaction of chemical compounds from building materials.

In this section, we report the development of a flat plate type test chamber (FPT chamber) that can be used to obtain the mass accommodation coefficients (γ) of ozone depositing to different surface materials. The purpose of this study is to develop a numerical method based on Computational Fluid Dynamics (CFD) to predict the ozone distribution in a room. More specifically, this study is designed to develop a reliable method, using a flat plate type test chamber (FPT chamber), to examine ozone deposition on building materials, and to estimate the mass accommodation coefficients of ozone, which are a fundamental parameter of the surface deposition flux model for ozone.

2.1 Modelling the Wall Surface Deposition Flux of Ozone

The surface deposition of the local concentration close to the surface and, from molecular theory, the flux at the surface is given by [Cano-Ruiz et al., 1993]:

$$Js = -\gamma \frac{\langle v \rangle}{4} C_o\big|_{y=\frac{2}{3}\lambda} \qquad (2\text{-}1)$$

Here, γ [-] is the mass accommodation coefficient; $<v>$ [m/s] is the Boltzmann velocity for ozone; and λ [m] is the mean molecular free path of ozone (6.5×10^{-8} [m]).

2.2 Outline of Flat Plate Type Test Chamber and Its Conditions

Figure 2-1 shows a perspective layout of the FPT Chamber and a photo of its external appearance. The FPT chamber is a channel cavity measuring 2,000(x) ×300(y) ×10(z) [mm] in which a two-dimensional mean flow field is developed. The FPT chamber consists of three sections, a running-section (300(x) [mm]), a test-section (1500(x) [mm]), and a running-section (200(x) [mm]). It is equipped with 10(z) [mm] width inlet and outlet slots. The four boundaries – ceiling, floor, right, and left walls – are made of glass. The deposition of ozone onto glass is known to be comparatively small [Cano-Ruiz et al., 1993] and is neglected.

The air inlet velocity (U_{in}) was set at 1.0 [m/s] (air change rate: 2400 [times/h]). The inlet air and all the walls were maintained at isothermal conditions (293 ± 1.0 [K]). The supply air was passed through activated carbon and HEPA filters to keep the concentration of background contaminants low. In order to prevent photochemical reactions involving ozone, the FPT chamber experiments were carried out in a darkroom. The points of measurement

in the FPT chamber are shown in Figure 2-1 (Positions (1) – (4)). The height of the floor of the FPT chamber is adjustable in proportion to the thickness of the target building materials to accurately maintain the 10 [mm] height in the *z* direction.

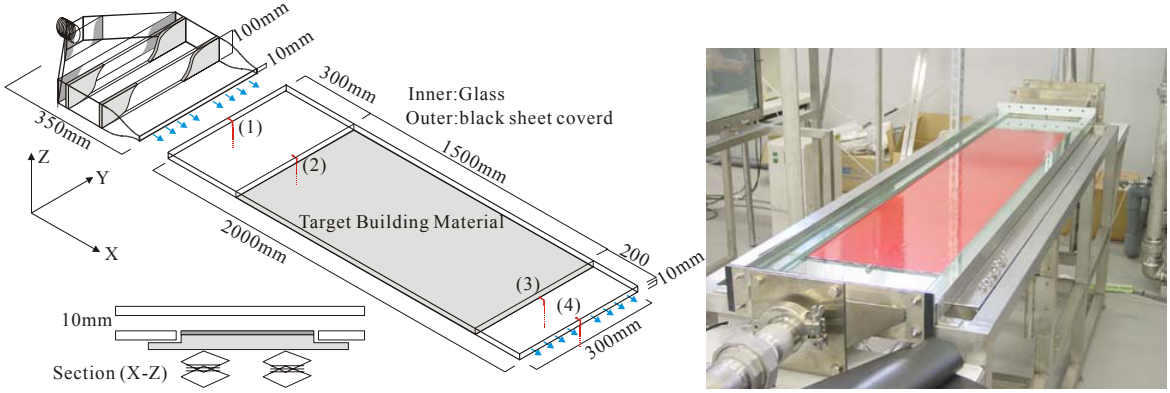

Figure 2-1 Perspective layout and photo of FPT Chamber

2.3 Measurement Data and Method

In this experiment, the target chemical compound was ozone. Ozone was introduced into the supply airflow at a constant concentration of 1.000 [ppm]. Ozone was analyzed using a UV Photometric Analyzer at a wavelength of 254 [nm]; its concentration range was 0 - 9.999 [ppm], and its precision was 0.001 [ppm]. The sampling flow rate of the UV Photometric Analyzer was 1.5 [L/min] and the ozone concentration was calculated as a time-averaged concentration over ten minutes. GC/MS and HPLC were used for the background volatile organic compounds (VOCs) and aldehydes. A digital dust concentration analyzer (light scattering method) was used to monitor background Suspended Particulate Matter (SPM).

This experiments focused on the heterogeneous reactions between ozone and various building materials, which are assumed to occur at the wall surfaces set at the floor level in the FPT chamber. Seven building materials; stainless steel (SUS 304), water- and oil-based paints, wallpaper, plywood, SBR rubber, and cedar were selected as test materials. Water- and oil-based paints were applied to the SUS 304 board with a coverage of 300 ± 15 [g/m^2] and allowed to dry. The experimental cases are shown in Table 2-1.

Table 2-1 Experimental cases

Exp. Case	Building Material	C_{in} [Ozone]	U_{in} ($=\overline{u}$)
Case (eb)	Glass	1.000 ppm	1.0 m/s
Case (e1)	SUS 304		
Case (e2)	Water-based paint		
Case (e3)	Oil-based paint		
Case (e4)	Wallpaper		
Case (e5)	Plywood		
Case (e6)	SBR rubber		
Case (e7)	Cedar		

2.4 Results of Experiment

Mean Velocity

The Reynolds number at the supply inlet position is *Re*=700 (U_{in}=1.0 [m/s], L_{in}=10 [mm]=channel height (*z*)) and hence a laminar flow field is generated in the FPT chamber. Figure 2-2 shows the vertical and horizontal profiles of U_{in} as measured by a thermistor anemometer. Constant flow distributions are formed at the supply inlet position.

Figure 2-3 shows the vertical flow patterns along the *x* direction (downstream direction) based on a laminar flow analysis. The analysis, in which a constant flow distribution is given as a boundary condition at the supply inlet position, establishes that fully-developed and constant laminar flow profiles are generated at the test section (x>300 [mm]).

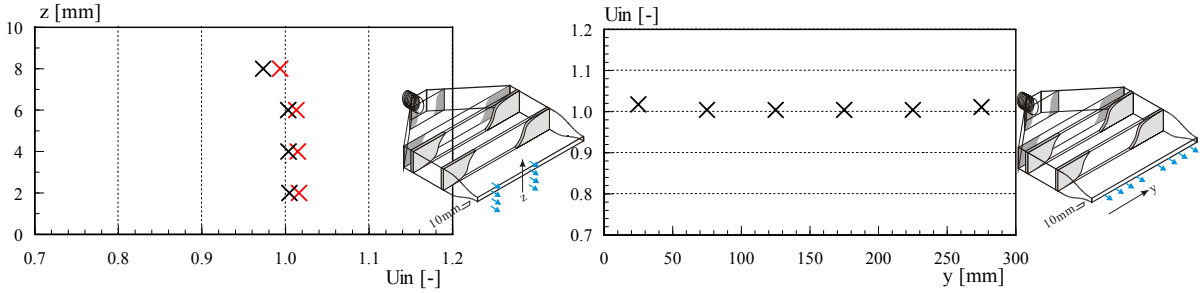

(1) Vertical Profile of U_{in} (2) Horizontal Profile of U_{in}

Figure 2-2 Flow field at supply inlet

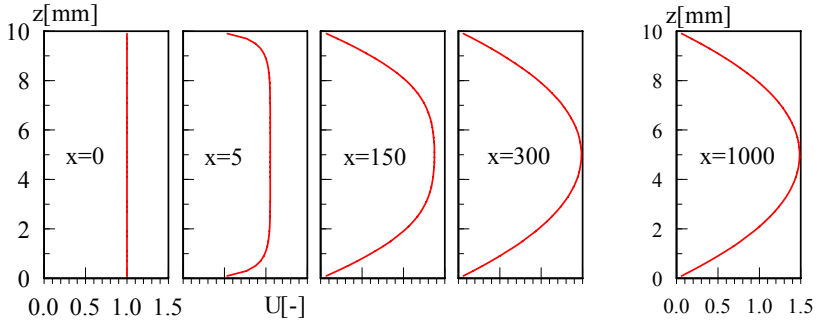

Figure 2-3 Vertical flow patterns along the *x* direction (downstream direction)

Background Concentration

The background concentration of the sum of the airborne organic compounds was confirmed to be below 30 [μg/m^3], while the Suspended Particulate Matter (SPM) in the supply air was 0.01 [mg/m^3] (total concentration of particles of diameter 10μm or less). Hence, uni- and bi-molecular chemical reactions of ozone in the air phase were negligible in the FPT chamber experiment.

Ozone Concentration

Table 2-2 shows averages for the measured ozone concentrations at sampling position (4). Ozone concentration measurements were conducted in triplicate for each target building material. In these experiments, target building materials were set up on the floor (1-sided deposition) in the FPT chamber. Ozone concentrations at sampling position (4) are normalized to the supply inlet concentration of ozone (C_{in}). In Case (eb), which estimates the background deposition onto the glass surface in the FPT chamber, the ozone concentration reduction at position (4) after passing over the target building material was less than 1 %. Hence, it was confirmed that the background ozone deposition in the FPT chamber was negligible. Among the evaluated building materials, plywood produced the maximum reduction in ozone concentration.

Table 2-2 Ozone concentration and estimated mass accommodation coefficient (γ)
(1-sided deposition)

Exp. Case	C_{in} (Sampling Position (1))	Concentration at Sampling Position (4)	γ [-]
Case (eb)	1.000 [ppm]	0.999	$< 1.1\times10^{-7}$
Case (e1)		0.954	3.4×10^{-6}
Case (e2)		0.934	4.9×10^{-6}
Case (e3)		0.921	6.1×10^{-6}
Case (e4)		0.968	2.3×10^{-6}
Case (e5)		0.894	8.7×10^{-6}
Case (e6)		0.920	6.2×10^{-6}
Case (e7)		0.932	5.2×10^{-6}

Table 2-3 shows the average measured ozone concentrations at sampling position (4) in the case of 2-sided deposition (target building materials are set up both on the ceiling and the floor). When SUS 304 (Case (e1)*) was evaluated, the ozone concentration was significantly reduced compared with Case (e1) for 1-sided deposition.

Table 2-3 Ozone concentration and estimated mass accommodation coefficient (γ)
(2-sided deposition)

Exp. Case	C_{in} (Sampling Position (1))	Concentration at Sampling Position (4)	γ [-]
Case (eb)	1.000	0.999	$< 1.1\times10^{-7}$
Case (e1)*		0.903	3.7×10^{-6}

2.5 Estimation of Mass Accommodation Coefficient

The equations governing ozone transport are shown in Table 2-4 under the conditions of a fully-developed two-dimensional laminar flow field with diffusive streamwise transport neglected.

The governing equations in Table 2-4 were used to calculate the average concentration of ozone at the outlet of the test section (i.e. the concentration after passing over the surface material) as a function of the mass accommodation coefficient (γ); the results are shown in Figure 2-4. The calculations were carried out for both 1-sided deposition and 2-sided deposition. Using the data for the average concentration of ozone as a function of γ, values of γ were estimated directly from the experimental results, and are shown in Tables 2-2 and 2-3.

Table 2-4 Equations governing ozone transport in the FPT chamber (1-sided deposition)

$$\frac{3}{2}\overline{u}\left[\left(\frac{z}{h}\right)^2-1\right]\frac{\partial C}{\partial x}=D_o\frac{\partial^2 C}{\partial z^2},\ -h\le z\le h,\ 0\le x\le x_L \qquad (1)$$

$$J=D_o\frac{\partial C}{\partial z}=\gamma\frac{\langle v\rangle}{4}C \quad \text{at} \quad z=-h \qquad (2)$$

$$\frac{\partial C}{\partial z}=0 \quad \text{at} \quad z=h \qquad (3)$$

$$C=C_{in} \quad \text{at} \quad x=0 \qquad (4)$$

x_L : length of test section (=1500mm)
h : half width of channel height (=5 mm)
C_{in} : supply inlet concentration of ozone (=1.000 ppm)
$\overline{u}$: supply inlet velocity (=1.0 m/s)
D_o : molecular diffusion coefficient of ozone ($=1.81\times10^{-5}$ m^2/s)
<v> : Boltzmann velocity (= 360 m/s)

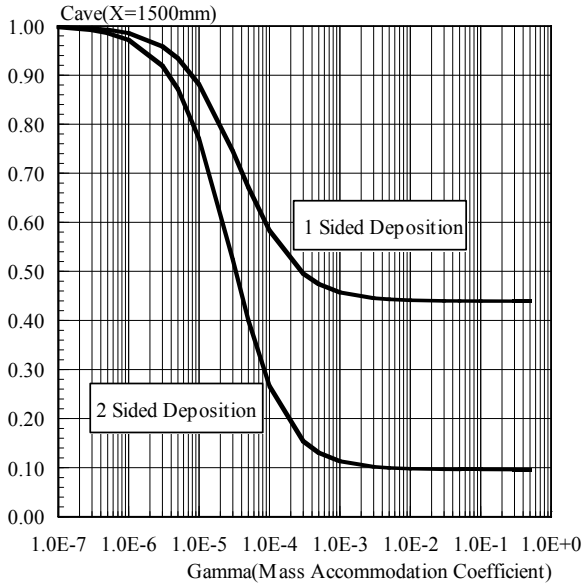

Figure 2-4 Average concentrations at the outlet of the test section (C_{ave}) for various γ values

The γ value was estimated to be below 1.1×10^{-7} [-] for Case (eb), which used glass as the target deposition material. The γ values become larger in proportion to the reduction in the ozone concentration. The γ values for the seven building materials were estimated to be between 8.7×10^{-6} [-] (Case (e5) for plywood) and 2.3×10^{-6} [-] (Case (e4) for wallpaper).

2.6 Discussion

For 2-sided deposition, the reduction in the ozone concentration is larger than that for 1-sided deposition for the same building material. Hence, the uncertainty of the concentration measurement for 2-sided deposition is much

smaller than for 1-sided deposition. The estimated γ value for SUS 304 for 1-sided deposition (Case (e1)) was 3.4×10^{-6} [-] and for SUS 304 for 2-sided deposition (Case (e1)*) was 3.7×10^{-6} [-] as shown in Tables 2 and 3. In this experimental setup, the estimation error between 1-sided and 2-sided deposition is about 8%, and it was confirmed that the measurement and estimation were sufficiently accurate.
Other studies (Cano-Ruiz et al., 1993; Morrison and Nazaroff, 2002) indicate that, for some materials, the γ value is likely to become smaller as the material is exposed to ozone for longer periods of time. This topic will be the subject of future experiments.

3. INDOOR AIR BIOLOGY

During the past decade, considerable progress has been made on understanding and controlling fungal growth in buildings. Studies in many countries have recognized the association between respiratory symptom, moisture problems, and fungal growth in buildings. In other words, fungal growth and infestation in buildings causes allergic diseases, asthma and rhinitis.
Though a lot of researches concerning fungal growth have been conducting, the harmful influence of fungal growth and infestation cannot be detected directly and it is very difficult to predict quantitatively the fungal growth and its impact to human health.
The fungal growth and infestation are deeply associated with indoor air humidity, temperature, building materials and ventilation rate. The final goal of this study is to develop the numerical model that predict microorganism growth and MVOC emission by taking into account the influence of moisture, temperature and building materials. The microorganism growth model and diffusion model of airborne fungi will be incorporated into CFD simulation.

In this section, the study focuses on the fungal contamination among various factors affecting the indoor environment. Its final goal is to develop a method to predict the emissions of chemical substances from microorganisms and the growth and proliferation of microorganisms. The following specifically reports on the results of measuring microbial volatile organic compounds ("MVOC") emitted from the following three species of fungi: *Alternaria*, *Eurotium*, and *Aspergillus*.

3.1 Experimental Method

Indoor concentration levels of MVOC are extremely low and it is difficult to measure them by an ordinary detection method. In the experiment, therefore, a chamber enabling low concentration MVOC sampling was developed to measure MVOC emitted from each of the three species of fungi.

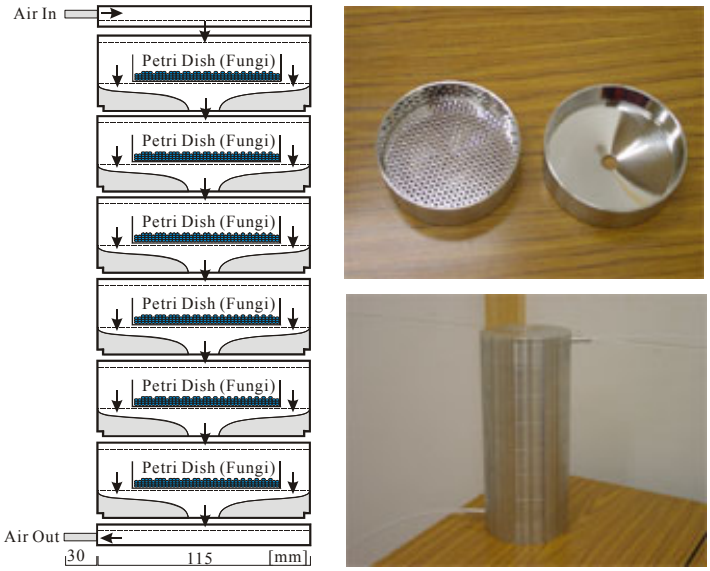

Figure 3-1 Small Cell Type Chamber

The chamber for measuring MVOC was composed of six SUS304 stainless steel units placed one on top of another. The cylinder-shaped units, each with an inside diameter of 110×10^{-2} [m] and a depth of 37×10^{-2} [m], allowed air to circulate vertically. These units were designed to be hermetically closed without the use of sealing materials. Figure 3-1 shows the chamber for measuring MVOC and the outer and inner appearances of the units comprising this chamber. Also, Figure 3-1 shows the experiment system used for measuring MVOC.

N2-based O2 (20%)-blended gas (P>99.99999) was used as the air to be supplied to the chamber, and the relative humidity was set at 0%. Activated carbon-based chemical filters were placed at two points on the upstream side to clean the air supplied to the chamber. The supply volume was controlled at 350 [cc/min] by a mass flow controller.

3.2 Fungal Strains Used for the Experiment

Among fungi that are confirmed to generally exist indoors, three species were chosen for the experiment: one species that thrives at high humidity; one that thrives at medium humidity; and one that can thrive even at low humidity. The National Institute of Technology and Evaluation (NITE) Biological Resource Center (NBRC) provided all fungal strains of these three species. Specifically, *Alternaria alternata* (NBRC 31805) (Case1); *Eurotium herbariorum* (NBRC 33235) (Case2); and *Aspergillus penicillioides* (NBRC 33024) (Case3) were used in the experiment. *Eurotium herbariorum* thrives at low humidity and is known to grow faster at the relative humidity of 73%–95%. *Alternaria alternata* thrives at high humidity and is known to grow faster at the relative humidity of 96% or higher. *Aspergillus penicillioides* can thrive even at very low humidity and grows better at low humidity than *Eurotium* and *Alternaria*.

Table 1 lists the fungal strains used in the experiment and outlines the culture conditions. The fungi to be placed inside the units were first inoculated onto PDA culture media using glass Petri dishes. After being cultured for 10 days in an incubator set at a constant 28℃, they were placed inside the units, one in each unit (six in total). *Eurotium herbariorum* thrives at high osmolarity and needs sugar for proliferation. Glucose was therefore added to the culture media (at 30% of the total).

3.3 Sampling and Analysis Method

On the downstream side of the chamber for measuring MVOC, active sampling was conducted targeting the air passing through the chamber which contained MVOC by the use of Tenax TA (Gestel, 80/100 mesh). A pump with a flow volumeter was used for the sampling of 500 [L] in total at the rate of 350 [cc/min]. The sampling was conducted two consecutive times to confirm the reproducibility and time series changes. The qualitative and quantitative analyses were conducted by gas chromatography/mass spectrometry (GC/MS).

Table 3-1 Analysis Conditions for MVOC

GC/MS	HP6890
TDS	Gestel TDS (Thermal Desporption System)
Column	HP5 (0.25mmϕ×60m×1μm)
Oven Temp.	40°C(3min)→10°C/min→220°C(10min)
Detector	HP5973MSD
Sampler	Tenax TA (60/80 mesh)
Sampling Speed	350 cc/min, Total 500 L

3.4 measurement of Background VOC revels

In order to identify the levels of background VOCs containing similar groups as MVOC, in addition to confirming the emission of background chemical substances from the supplied air and the experiment system, sampling was also conducted under blank conditions (with only PDA culture media and a glass Petri sheet). It was confirmed that the levels of MVOC components identified in previous studies were at or lower than the detection limits and the other background VOC levels were also at ignorable levels.

3.5 Results

Figure 3-2 shows the measurements of MVOCs emitted from each of the fungal strains in the form of a chromatograph.

(1) *Aleternaeia alternata* (Case 1)

As an MVOC, 3-octanone was identified. The MVOC emission from Aleternaeia alternata was the lowest among all of the experiment cases. There is a possibility that *Aleternaeia alternata*, which thrives at high humidity, could not grow and proliferate during the experiment, in which the relative humidity of the air to be supplied was set at 0%, which in turn resulted in the low MVOC emission.

(2) *Eurotium herbariorum* (Case 2)

As MVOC from *Eurotium herbariorum*, four types (3-methyl-1-butanol, 1-octen-3-ol, 3-octanone, and 3-octanol) were identified. There is a possibility that *Eurotium herbariorum*, which thrives at high osmorality, grew and pro-

liferated because of the glucose added to the culture media, which in turn contributed to an increase in the types of MVOC and in the emission level.

(3) *Aspergillus penicillioides* (Case3)
As MVOC from *Aspergillus penicillioides*, 1-octen-3-ol and 3-octanone were identified. Samplings were consecutively conducted to measure time series changes, and the emission levels were almost the same in all the samplings. Although the humidity set for the experiment was not optimal for the growth of *Aspergillus penicillioides*, this fungus can even thrive at very low humidity. Therefore, there is a possibility that it grew and proliferated to a certain degree during the sampling period, which in turn resulted in the constant emission of MVOC

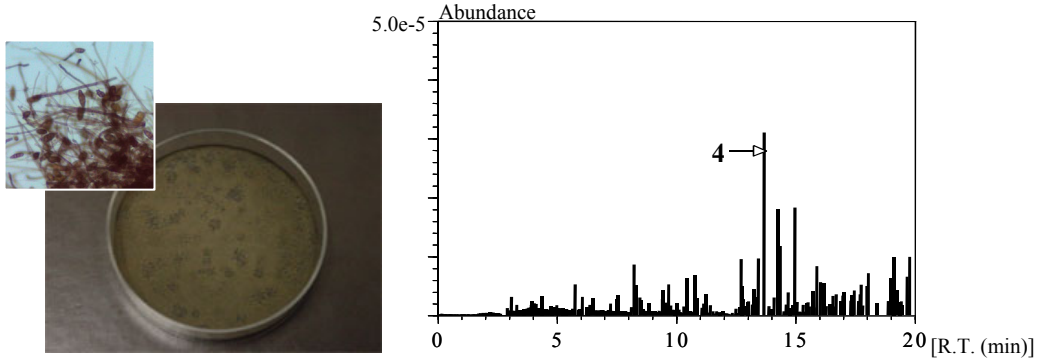

(1) *Aleternaeia alternata*

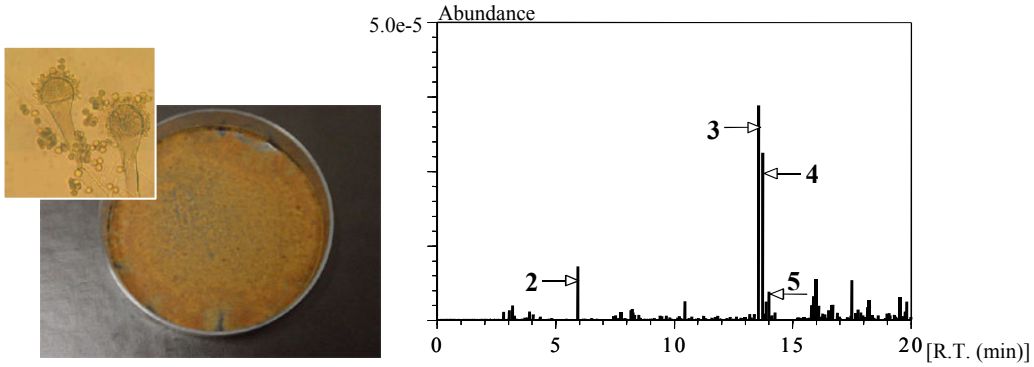

(2) *Eurotium herbariorum*

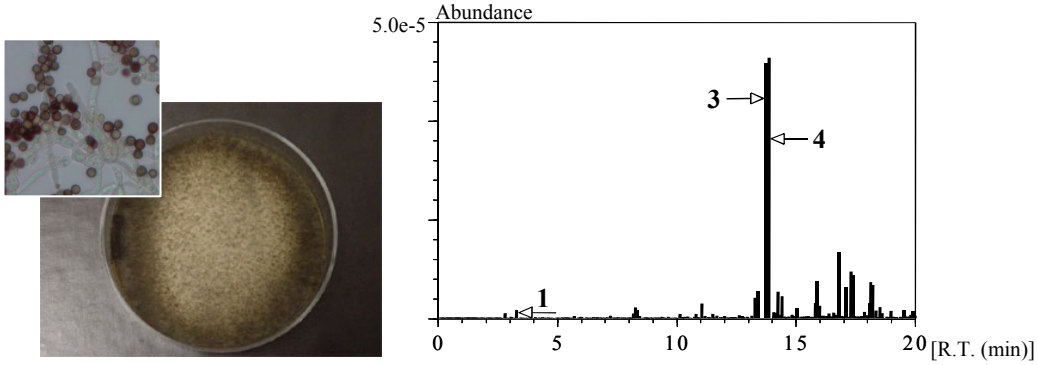

(3) *Aspergillus penicillioides*

Figure 3-2 Total Ion Chromatogram of MVOC Components

Table 3-2 MVOC (Microbial Volatile Organic Compound) detected

Number	MVOC
1	2-pentanol
2	3-methyl-1-butanol
3	1-octen-3-ol
4	3-octanone
5	3-octanol

3.6 Considerations

The emission of MVOC was confirmed for all the species of fungi used in the experiment. Compared with various MVOC identified in previous studies, those identified in the experiment have relatively large molecular weights. All of these substances had peaks later in the analysis method (delayed R.T). In the analysis method used this time, therefore, hydroxyl group-containing MVOC having relatively low molecular weights might be purged. Examinations should be made regarding this issue.

In the experiment, MVOC were measured only at the atmospheric temperature of 28℃ and at the relative humidity of 0 %. It is, however, necessary to measure MVOC at the optimal temperature and humidity for the growth of each targeted fungus and thereby to measure MVOC emissions in consideration of the fungal metabolism.

4. INDOOR AIR PHYSICS

In recent years, numerical simulation of airflow, temperature and contaminant distribution is used in the design of room air- conditioning or of indoor air quality. It is effective in analyzing the structure of the contaminant distribution field and can be used to design a precise controlling method. An important goal in research on the indoor environment is an enhanced understanding of the mechanisms responsible for human perception to different exposures. CFD (Computational Fluid Dynamics) may be used to obtain detailed information about flow field and distributions of temperature and concentrations inside a room and particularly in the close vicinity of a person.

A detailed numerical analysis of thermal comfort in various parts of the human body and air quality in the breathing zone requires the development of computer simulated person (virtual manikins) representing in detail human body shapes as well as physiological phenomena. A series of studies including the one described in this report aim to develop virtual manikins that represent various human body scales and human body shapes as well as incorporate a comfort equation routine allowing the control of skin surface temperature, and to create a grid library of virtual manikins in a data format that is readily applicable to a detailed computational fluid dynamics (CFD) analysis of microclimates around the human body.

In this section, we report the development of Virtual Manikins for CFD analysis applications. Particularly, this report describes the results of our development of standing and seated virtual manikins representing a human body scale for seven-year-olds (child model), as well as results of our investigation of the accuracy of indoor environment prediction, which was conducted on a simple room using a coupled analysis of convection and radiation.

4.1 Previous Studies with regard to development of Computer Simulated Person

Currently indoor environment studies focus on phenomena around the human body at the microclimate level, and therefore the need for more realistic and detailed human body models has been pointed out. Numerical models representing closely the actual shape of the human body have already been proposed for seated female models (or androgynous models based on female body shapes), and are available for indoor environment analysis applications. However, other human body shapes have not been modelled. In addition, since existing models use coarse meshes, sufficient detailed data on various parts of the human body has not been gathered.

4.2 Development of Virtual Manikins

This study aims to develop virtual manikins that represent human body scales for adult males and females as well as child (almost seven-year-olds). This report provides an overview of the development of models for seven-year-olds child. The virtual manikins developed in this study cover two types of posture models (a seated model in Figure 4-1 (1), and a standing model in Figure 4-1(2)). The geometric shapes of ears and fingers (Figure 4-2) are also represented for a detailed representation of the human body. Table 4-1 shows information on each human body model. The surface area is about 0.85 [m^2] for each model. The smallest mesh size for the surface of the human body is assigned to the face in both models and is 0.49 [mm^2]. The total number of meshes is limited to about 20,000 to prevent an excessive increase in the number of meshes assigned to the space. The virtual manikin is divided into 17 parts for the control of the thermal manikin, allowing the control and analysis of radiation heat transfer, surface temperature, and other factors in each part.

4.3 Fanger's Equation

A routine that determines the skin temperature as the convergence value for the ambient environment and heat exchange was incorporated in the virtual manikins in this study. Equation (4-2) is obtained by rearranging the heat balance Equation (4-1) in the thermally neutral conditions proposed by Fanger et al. This virtual manikin aims at thermal neutrality. Heat balance at the boundary of the human skin surface is controlled by generating heat in proportion to the discrepancy between the thermally neutral temperature of 36.4 [°C] of the human body and the current skin temperature T_{sk} [°C].

$$T_{sk} = 36.4 - (0.054 + R_{cl})Q_t \quad (4\text{-}1)$$

$$Q_t = \frac{1}{(0.054 + R_{cl})}(T_{sk} - 36.4) \quad (4\text{-}2)$$

Where Q_t is the amount of sensible heat radiated (W/m^2) and R_{cl} is the amount of heat transferred through clothing (m^2K/W).

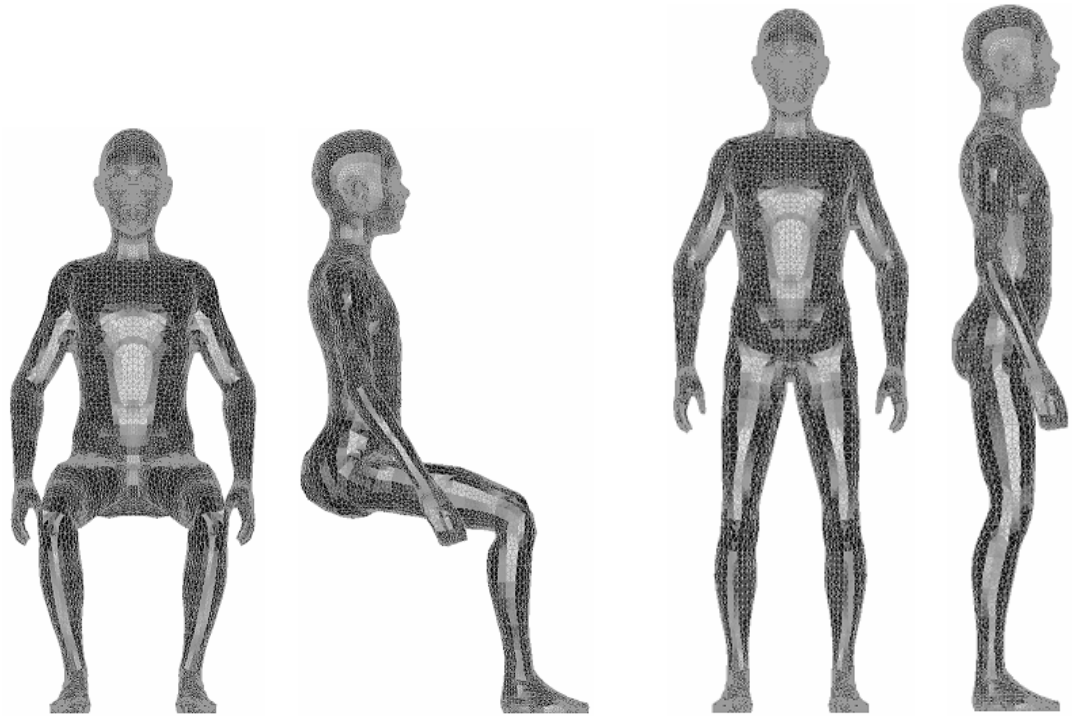

(1) Seated model (2) Standing model

Figure 4-1 Virtual Manikin (Child Model)

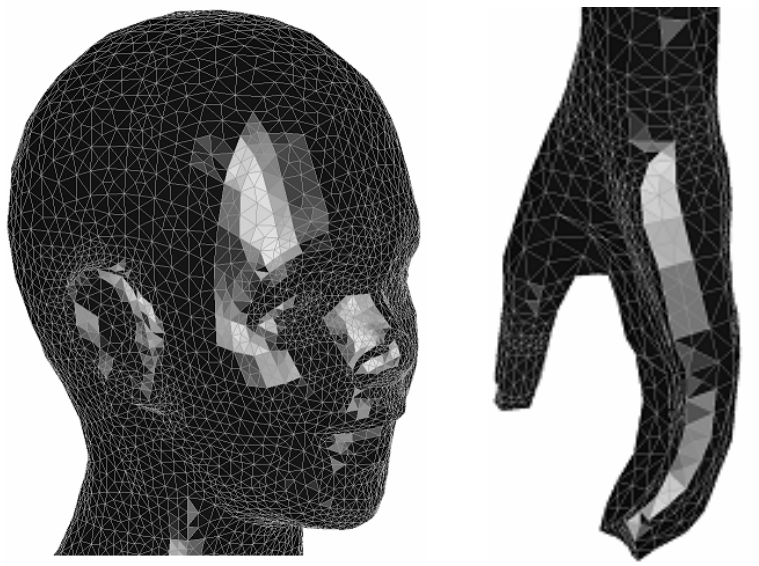

Figure 4-2 Zoom of the face and hand

Table 4-1 Surface Area of the Individual Segment of the Manikin (Child Model)

Segment	Seated Model (Child, 7 years)	Standing Model (Child, 7 years)
Area of Whole body [m^2]	0.848	0.847
Volume of Whole body [m^3]	0.022	0.022
Smallest Surface Mesh Size [mm^2]	0.490	0.490
Largest Surface Mesh Size [mm^2]	154.933	151.715
The Number of Surface Mesh	20085	18971
Area of left and right Foot [m^2]	0.023	0.023
Area of left and right Leg [m^2]	0.063	0.060
Area of left and right Thigh [m^2]	0.079	0.071
Area of left and right Hand [m^2]	0.019	0.019
Area of left and right Arm [m^2]	0.030	0.030
Area of left and right Shoulder [m^2]	0.035	0.037
Area of Pelvis [m^2]	0.102	0.123
Area of Chest [m^2]	0.079	0.079
Area of Back [m^2]	0.073	0.068
Area of Face [m^2]	0.036	0.036
Area of Neck [m^2]	0.059	0.059

4.4 Coupled Analysis of Convective and Radiation Heat Transfer

CFD analysis is based on analysis by the low-Reynolds Number Type k-ε model (Abe-Nagano model) in order to represent the flow patterns in the viscous sub-layer near wall surface. The effect of temperature on density change was evaluated, using the ideal gas equation with the assumption of constant pressure. A steady-state analysis was carried out, using the SIMPLE method as the calculation algorithm, the QUICK scheme for advection term as the difference scheme, and a second order of center difference scheme for the others.

In radiation analysis, the view factors were obtained by the Discrete Transfer method, and mutual-radiation characteristics in the space are analyzed using the Radiosity Method. Indoor air temperature distributions and the amount of heat transferred by convection on the skin surface Q_{ci} were calculated by CFD analysis, using the skin temperature T_{sk}. Radiation heat transfer analysis (Q_{Ri}) was carried out as well, using T_{sk} at this point. The total heat flux Q_{Ti} was calculated by adding Q_{Ci} and Q_{Ri}. This was sent to the comfort equation routine (routine of Fanger's equation). These steps were repeated until the quantities converged.

Table 4-2 Numerical and Boundary Conditions

Turbulence Model	Low Re type k-ε model (Abe-Nagano Model, 3-dimensional calc.)
Scheme	Convection Term: QUICK
Inflow Boundary	U_{in} = 0.1 [m/s], Area of Supply Inlet 300×300[mm] k_{in} =3/2× (U_{in}×0.05)^2 , ε_{in} =C_μ×$k_{in}^{3/2}$/l_{in}, C_μ=0.09, l_{in} =(Slot width) ×1/7
Outflow Boundary	U_{out} = Free slip, k_{out}= Free slip, ε_{out} = Free slip T_{in} = 273 [K]
Wall Treatment	Velocity: No slip $k\big\|_{wall}$: No slip， $\varepsilon\big\|_{wall} = 2\nu(\partial\sqrt{k}/\partial y)^2$ Temperature: Adiabatic condition Emissivity: 0.9
Surface Treatment of Virtual Manikin	Velocity: No slip $k\big\|_{wall}$: No slip， $\varepsilon\big\|_{wall} = 2\nu(\partial\sqrt{k}/\partial y)^2$ Temperature: Fanger's Equation Emissivity of Radiation: 0.9

4.5 Outline of the Benchmark Test

A benchmark test was carried out on a simple room to examine the accuracy of indoor environment prediction with the virtual manikin developed in this study. Figure 4-3 shows the analysis model. The virtual manikin was placed in the middle of the room to be analyzed with a special scale of x = 3.2 [m], y = 3.2 [m], z = 2.8 [m]. About

950,000 meshes were created for the seated model, and about 960,000 meshes for the standing model. Figure 4-4 shows the grid design for the surroundings of the virtual manikin. Triangular meshes were assigned to the human body surface, prism meshes to the first to the fourth cell from the human body surface to the fluid, and tetra meshes to the fifth cell to the interior wall of the room. The non-dimensional distance in the normal direction (wall unit) y^+ between the human body surface and the center of the first grid point met the condition $y^+ < 0.1$ in all parts of the human body.

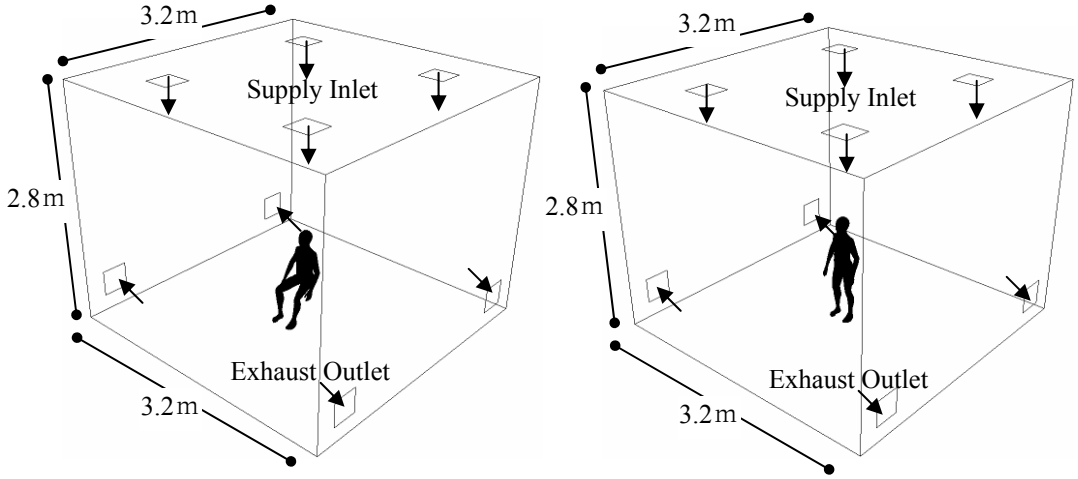

(1) Sitting Position (2) Standing Position

Figure 4-3 Model Room Analyzed

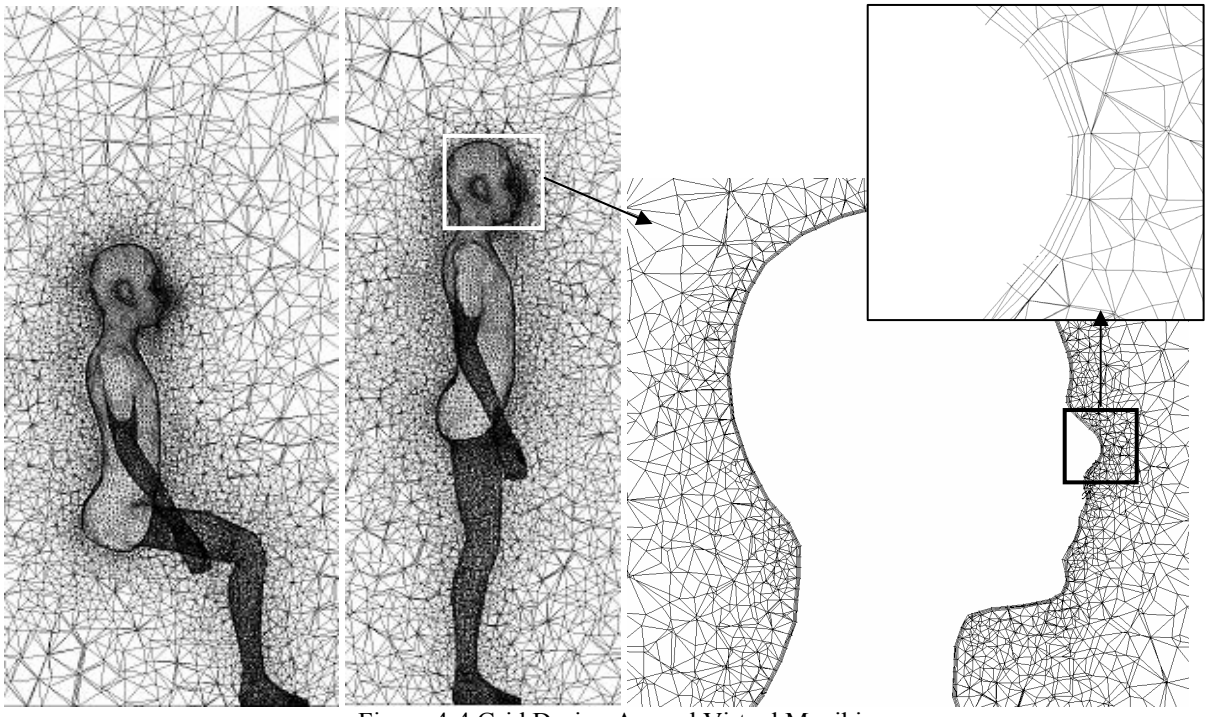

Figure 4-4 Grid Design Around Virtual Manikin

4.6 Analysis Results

4.6.1 Analysis Results of Velocity Distribution

Figures 4-5 show the results of the flow-field analysis. The heat flow from the human body formed a thermal up-flow around it. The thermal upflow was formed in the direction from the foot to the head, and broke away from the surface at the thigh, hip, and flank in the seated model and at the groin, flank, and jaw in the standing model. At the top of the head of the virtual manikin, a thermal upflow with a maximum velocity of about 0.25 m/s was formed.

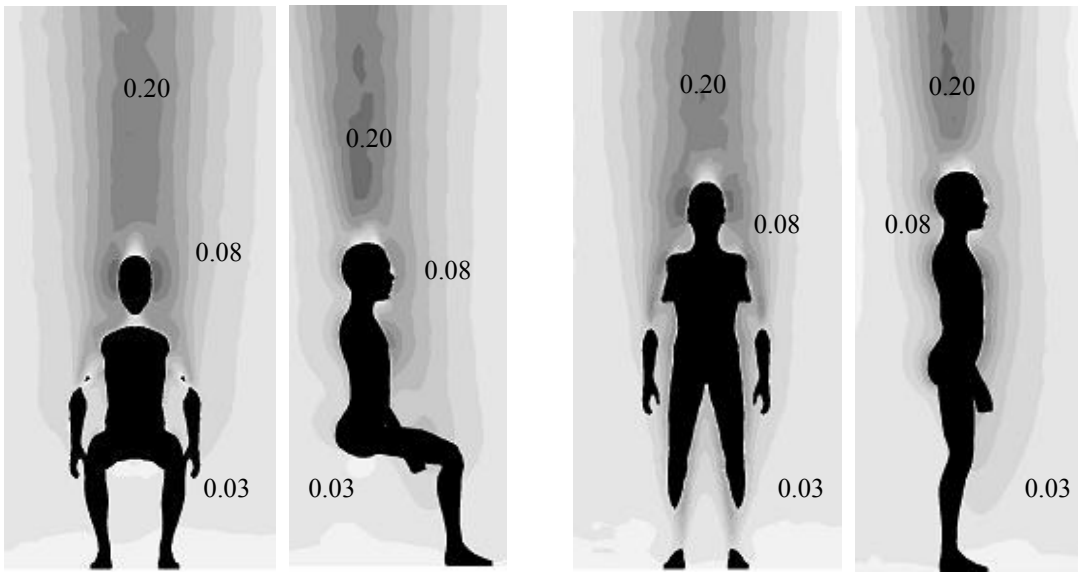

(1) Sitting Position (2) Standing Position

Figure 4-5 Distributions of Scalar Velocity around Virtual Manikin [m/s]

4.6.2 Analysis Results for Skin Surface Temperature Distribution

The skin surface temperature was controlled by the comfort equation routine, taking into account heat balance with the ambient environment. Figure 4-6 shows the skin surface temperature distribution. The temperature was about 35°C at the flank, groin, and hip, while it was about 33°C at the chest and abdomen.

4.6.3 Analysis Results for Radiation Heat Flux Distribution

Figure 4-7 shows the radiation heat flux distribution. The heat flux was the largest at the back in both models, with about 36 W/m^2. The flux was the smallest at the hand, with about 29 W/m^2 in the standing model and 26.5 W/m^2 in the seated model. The average radiation heat flux was 33.6 W/m^2 in the standing model and 31.9 W/m^2 in the seated model.

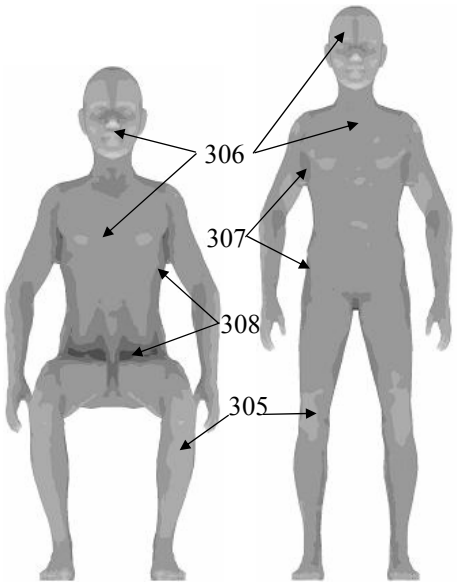

(1) Sitting Position (2) Standing Position

Figure 4-6 Surface Temperature Distributions [K]

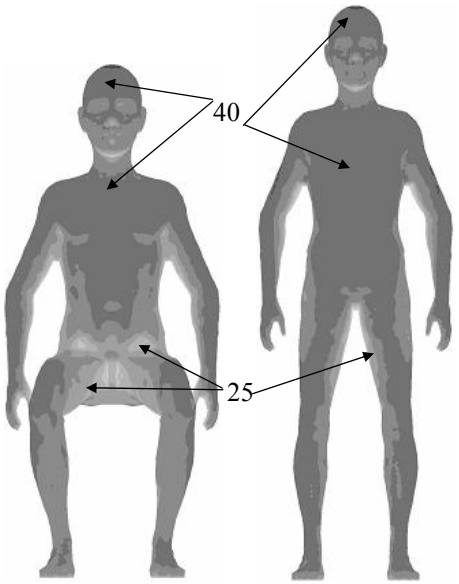

(1) Sitting Position (2) Standing Position

Figure 4-7 Radiation Heat Transfer Rate [W/m^2]

4.6.4 Analysis Results for Convection Heat Flux Distribution

Figure 4-8 shows the convection heat flux distribution. The heat flux was large at the hand in both models, with 35.3 W/m^2 in the standing model and 36.2 W/m^2 in the seated model. The heat flux was the smallest at the neck in both models, with about 20.4 W/m^2 in the standing model and 19.9 W/m^2 in the seated model. The average con-

vection heat flux on the human body surface was 27.0 W/m^2 in the standing model and 27.4 W/m^2 in the seated model.

4.6.5 Analysis Results for Total Heat Flux Distribution

Figure 4-9 shows the total heat flux distribution. The total flux was high at the nose and jaw, with about 100 W/m^2, in both models. The average total heat flux at the human body surface was 60.6 W/m^2 in the standing model and 59.3 W/m^2 in the seated model. These results are very close to actual phenomena, compared to statistical data on the average basal metabolism for seven-year-olds (57.4 W/m^2).

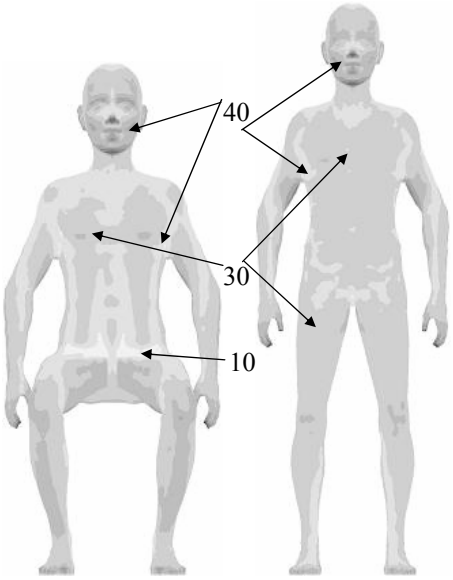

(1) Sitting Position (2) Standing Position

Figure 4-8 Convective Heat Transfer Rate [W/m^2]

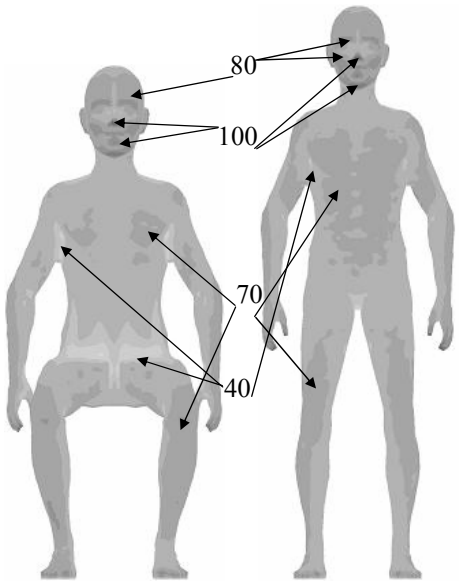

(1) Sitting Position (2) Standing Position

Figure 4-9 Total Heat Transfer Rate [W/m^2]

4.7 Discussion

In this report, we provided an overview of the development of virtual manikins for standing and seated postures representing seven-year-olds child. We examined the accuracy of indoor environment prediction by conducting a coupled convection and radiation analysis on a simple room. As a result, we confirmed that thermal environment prediction could be carried out with sufficient accuracy in the analysis of microclimates around the human body.

5. ESTABLISHMENT OF RESEARCH FIELDS OF PUBLIC HEALTH ENGINEERING

The objectives of this research is to develop procedure for coupled analysis of airflow, temperature, moisture distribution and pollutants diffusion field such as VOCs and microorganism, and finally to develop the comprehensive prediction method of IEQ (Indoor Environmental Quality) from the viewpoint of the engineering public health and to establish a paradigm for the integrated design of indoor environment that takes into account the Indoor Air Chemistry, Biology and Physics.

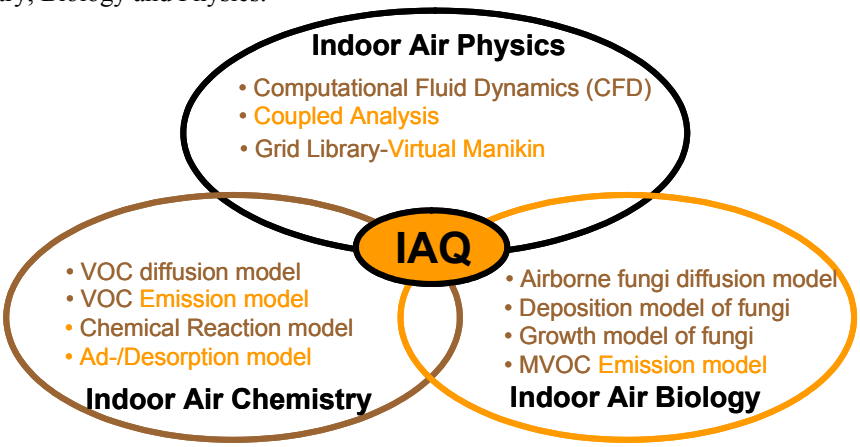

Figure 5-1 Research Diagram of Public Health Engineering

6. CONCLUSION

The objectives of our research are (1) to develop the fundamental model that predict emission, ad-/desorption and chemical reaction of VOCs (Indoor Air Chemistry), (2) to develop the numerical model that predict microorganism growth and MVOC emission by taking into account the influence of moisture and temperature (Indoor Air Biology), (3) to develop procedure for coupled analysis of flow, temperature, moisture and pollutants (Indoor Air Physics), and (4) to establish a paradigm for the integrated design of indoor environment that takes into account the Indoor Air Chemistry, Biology and Physics (Public Health Engineering). The research progresses until now are shown as follows;

With regard to INDOOR AIR CHEMISTRY;

- The flat-plate type test chamber was developed and the measurement of mass accommodation coefficient of ozone and sticking coefficient of HCHO were carried out for various building materials.
- The medium scale type test chamber (V=1.5 m^3) was developed and the measurement of VOCs emission rate from DIY furniture is conducting.
- Measurements of ozone concentration distribution in a model room with 2D flow field were completed.

With regard to INDOOR AIR BIOLOGY;

- The experimental setup was completed and the measurement of growth responses of fungi is conducting for various building materials by taking into account the influence of moisture and temperature.
- The micro cell type test chamber was developed and measurement of MVOC emission rate from various fungi (*Alternaria*, *Eurotium* and *Aspergillus*) were conducted by taking into account the influence of moisture and temperature.

With regard to INDOOR AIR PHYSICS;

- Coupled simulation of emission, diffusion and wall surface deposition (uni-molecular reaction) based on CFD simulation was carried out and the correspondence with the experimental results was verified.
- The gird library of Virtual Manikin in which takes into account various attitude, gender and comfort model are developing for coupled CFD simulation around human body (Analysis for micro-environment).
- Coupled simulation of emission, diffusion, ad-/desorption and chemical reaction (uni-molecular reaction) based on CFD simulation was carried out.
- The predictive accuracy of coupled CFD simulation was verified by comparing with the experimental data.

REFERENCES

[1] Altshuller AP and Wartburg AF (1961). The Interaction of Ozone with Plastic and Metallic Materials in a Dynamic Flow System. Int. J. Wat. Pollut. *4*, pp. 70-78.

[2] Cano-Ruiz JA, Kong D, Balas RB, Nazaroff WW (1993). Removal of Reactive Gases at Indoor Surfaces: Combining Mass Transport and Surface Kinetics. Atmospheric Environment *27*A (13), pp. 2039-2050.

[3] Cohen IC, Smith AF and Wood R (1968). A field method for the determination of ozone in the presence of nitrogen dioxide, Analyst *93*, pp 507-517

[4] Morrison GC and Nazaroff WW (2002). The rate of ozone uptake on carpet: mathematical modeling. Atmospheric Environment *36*, pp. 1749-1756

[5] Sabersky RH, Sinema DA, and Shair FH (1973). Concentrations, Decay Rates and Removal of Ozone and Their Relation to Establishing Clean Indoor Air. Envir. Sci. Technol., *7*, pp. 347-353.

[6] Simmons A and Colbeck I (1990). Resistance of Various Building Materials to Ozone Deposition. Envir. Technol., *11*, pp. 973-978.

[7] Sørensen DN and Weschler CJ (2002). Modeling Gas Phase Reactions in Indoor Environments Using Computational Fluid Dynamics. *Atmospheric Environment*, *36* (1): pp. 9-18.

[8] Weschler CJ (2000). Ozone in Indoor Environments: Concentration and Chemistry. Indoor Air *10* (4), pp. 269-288.

[9] Weschler CJ (2004). Chemical Reactions Among Indoor Pollutants: What We've Learned in the New Millennium. Indoor Air *14* (Suppl 7), pp. 184-194.

[10] Sorensen, D.N. and Voigt, L.K. (2003) Modelling flow and heat transfer around a seated human body by Computational Fluid Dynamics, Building and Environment, Vol.38, No.6, pp. 753-762

[11] Murakami, S., Kato, S., Zeng, J., (1997) Flow and Temperature fields around human body with various room air distribution, CFD study on Computational thermal manikin - part 1., ASHRAE Transactions, *103*, Part 1

[12] Topp C, Nielsen PV, Sørensen DN. (2002) Application of computer simulated persons in indoor environmental modeling, ASHRAE Transactions *108* (*2)* 1084-9

LIST OF PUBLISHED PAPER

[1] Kazuhide Ito, DN. Sørensen, CJ. Weschler : Measurements of Mass Accommodation Coefficients Using a Flat-Plate Test Chamber : *Indoor Air 2005*, The Tenth International Conference on Indoor Air Quality and Climate, Beijing, China, 2005 *(It is contributing*)

[2] Yuji Ataka, Shinsuke Kato, Shuzo Murakami, Qingyu Zhu, Kazuhide Ito, Tomohiro Yokota : Study of Effect of Adsorptive Building Material on Formaldehyde Concentrations: Development of Measuring Methods and Modeling of Adsorption Phenomena : International Journal of Indoor Air Environment and Health (*Indoor Air*), Volume 14, Supplement 8, 2004, pp 51-64
[3] Seohiro Kikuchi, Kazuhide Ito, Nobuyuki Kobayashi : Study on Normalized Concentration in an Occupied Zone in Office Space, Optimization of Supply Fresh Air Flow Rate and Analysis of Energy Consumption : *ROOMVENT2004*, Coimbra, Portugal, 5-8 September 2004, pp 48-49
[4] Kazuhide Ito, Shinsuke. Kato, DN. Sørensen, CJ. Weschler : Experimental and CFD Analyses Examining Ozone Distribution in a Model Room with a Two-dimensional Flow Field, 9th International Conference on Air Distribution in Rooms, *ROOMVENT2004*, Coimbra, Portugal, 5-8 September 2004, pp 234-235
[5] Shinsuke Kato, Kazuhide Ito, Shuzo Murakami, : Analysis of Visitation Frequency through Particle Tracking Method based on LES and Model Experiment : International Journal of Indoor Air Environment and Health (*Indoor Air*), Volume 13, No.2, 2003.6, pp 182-193
[6] Shuzo Murakami, Shinsuke Kato, Kazuhide Ito, Qingyu Zhu, : Modeling and CFD Prediction for Diffusion and Adsorption within Room with Various Adsorption Isotherms : International Journal of Indoor Air Environment and Health (*Indoor Air*), Volume 13, Supplement 6, 2003.1, pp20-27
[7] Kazukiyo Kumagai, Kazuhide Ito, Kiyoshi Takahara, Mikio Hashida, Hauipeng Tang, Yukio Yanagisawa : A Personal Air Purifier for School Children : *Healthy Buildings 2003*,Proceedings pp 610-615
[8] Seohiro Kikuchi, Kazuhide Ito, Nobuyuki Kobayashi : Numerical Analysis of Ventilation Effectiveness in Occupied Zone for Various Industrial Ventilation Systems : The 7th International Symposium on Ventilation for Contaminant Control, *VENT 2003*, Hokkaido, Japan, August 5-8 2003, pp103-108
[9] Nobuyuki Kobayashi, Kazuhide Ito, Robert N Meroney, Cheng-Hsin Chang : Measurement of contaminant concentration distribution by using image processing technique, 11th International Conference on Wind Engineering, *ICWE*, July 2003, pp2805-2812
[10] Kiyoshi Takahara, Mikio Hashida, Kazukiyo Kumagai, Kazuhide Ito, Yukio Yanagisawa : Back to School; Making of a "Personal Air Purifier For Schoolchildren's Chair" : *International Symposium on Indoor Air Quality and Health Hazards*, Japan, January 8 - 11, 2003, Poster Session
[11] Kazuhide Ito, Masaru Abuku, Shinsuke Kato, Shuzo Murakami : CFD and Model Experiment with Chemical Reaction : *International Symposium on Indoor Air Quality and Health Hazards*, Japan, January 8 - 11, 2003, Volume 1, pp305-311
[12] Nobuyuki Kobayashi, Seohiro Kikuchi, Yuji Takahashi, Kazuhide Ito : Numerical Analysis of Normalized Concentration in the Occupied Zone for Various Office Ventilation Systems: *ROOMVENT2002*, Copenhagen Denmark, September 8-11, 2002, pp129-132
[13] Shuzo Murakami, Shinsuke Kato, Qingyu Zhu, Kazuhide Ito : 3D-CFD Analysis of Diffusion and Emission of VOCs in a FLEC Cavity : *Indoor Air 2002*, The Ninth International Conference on Indoor Air Quality and Climate, Monterey, California, June 30 – July 5, 2002, pp548-543
[14] Shinsuke Kato, Shuzo Murakami, Qingyu Zhu, Kazuhide Ito : Measuring Methods of Reducing Effect of Pollutant Concentration with Adsorptive Building Material : *Indoor Air 2002*, The Ninth International Conference on Indoor Air Quality and Climate, Monterey, California, June 30 – July 5, 2002, pp658-663
[15] Kazuhide Ito, Shinsuke Kato, Shuzo Murakami, Qingyu Zhu : CFD Analysis of Chemically Reactive Pollutants in 2D Test Room : *Indoor Air 2002*, The Ninth International Conference on Indoor Air Quality and Climate, Monterey, California, June 30 – July 5, 2002, pp530-535
[16] Shuzo Murakami, Shinsuke Kato, Kazuhide Ito, Akira Yamamoto, Yasushi Kondo, Junichi Fujimura, : Chemical Pollutants Distribution in a Room Based on CFD Simulation Coupled with Emission / Sorption Analysis : *ASHRAE transaction* (Winter Meeting in Atlanta, January), 2001, AT-01-13-3
[17] Shuzo Murakami, Shinsuke Kato, Kazuhide Ito, Tatsuya Hayashi : CFD analysis of Indoor Chemical Environment and Inhaled Contaminant by A Human Body : The Third International Conference on Cold Climate Heating, Ventilating and Air- Conditioning, November 1-3, 2000, Sapporo, Japan
[18] Shuzo Murakami, Shinsuke Kato, Yasushi Kondo, Kazuhide Ito, Akira Yamamoto : VOC Distribution in a Room based on CFD Simulation Coupled with Emission / Sorption Analysis : *ROOMVENT 2000*, Reading, United Kingdom, July 9- 12, 2000, vol. 1, pp473-478
[19] Shuzo Murakami, Shinsuke Kato, Kazuhide Ito, Akira Yamamoto : Coupled Analysis of Emission, Sorption and Diffusion of Chemical Pollutants in Ventilated Room by CFD : *Indoor Air 99*, The 8th International Conference on Indoor Air Quality & Climate, Edinburgh, Scotland, August 8- 13, 1999, vol. 4, pp725-730
[20] Shuzo Murakami, Shinsuke Kato, Kazuhide Ito : Coupled Analysis of TVOC Emission and Diffusion in Ventilated Room by CFD : *EPIC'98*, Lyon, France, 19- 21 November, 1998、vol 1, pp19- 26